ORGANIC CHEMISTRY
FRONTIERS

RESEARCH ARTICLE

View Article Online
View Journal | View Issue

Cite this: *Org. Chem. Front.*, 2019, **6**, 110

Anion–π and anion–π-radical interactions in bis(triphenylphosphonium)-naphthalene diimide salts†

Chee Koon Ng, ‡[a] Teck Lip Dexter Tam, *‡[a] Fengxia Wei, [a] Xuefeng Lu[b] and Jishan Wu [b]

Received 17th October 2018,
Accepted 20th November 2018

DOI: 10.1039/c8qo01122b

rsc.li/frontiers-organic

We have conducted a systematic study of anion–π and anion–π-radical interactions in bis(triphenylphosphonium)-naphthalene diimide (BTPP-NDI) salts which was made possible with the synthesis of different anionic analogues. DFT calculations and experimental evidence show anion–π and anion–π-radical interactions and that the cationic π-radical can induce magnetic spin polarization of the anion.

Introduction

Anion–π interactions have been widely studied due to their potential applications in anion recognition,[1] ion transport,[2] catalysis[3] and anion doping.[4] Recently, organic π-radicals have also attracted academic interest due to their connection with polarons/solitons in the electrical and magnetic properties of doped conjugated polymers.[5] However, the nature of the interactions between the dopant/counter-ion and doped conjugated polymers is not well understood. In many cases, the doped conjugated polymers involve oxidized cationic or reduced anionic radical species that are chemically unstable towards air and/or water,[6] making the study of such interactions challenging. The recent advances in molecular design has enabled the syntheses of stable organic π-radicals.[7] Theoretical calculations on the influence of anion–π interactions on the magnetic spin polarization of the anion have also been reported.[8] Here we leverage on a stable bis(triphenylphosphonium)-naphthalene diimide (BTPP-NDI) cationic radical reported by Mukhopadhyay's group[7a] to study the effect of anion–π-radicals by systematic variation of the anion. We found that weakly Lewis basic anions are able to induce subtle red shifts in the solution UV-Vis absorption that is dominated by an optical transition from the cationic π-radical in the 1+ salts. Very weakly Lewis basic π-anions like NO_3^- interact strongly with the NDI π system *via* π–π interactions in the 2+ salt and behaves as an electron acceptor in the 1+ salt that can undergo photoinduced electron transfer (PET) from the radical cation to NO_3^-. The radical cation is also able to induce magnetic spin polarization of the anions as observed from NMR. Our results provide evidence for elusive anion–π-radical interactions and thus allow a better understanding of organic ferromagnets and p-doped conductors.

Results and discussion

Synthetic procedure

The syntheses of the BTPP-NDI compounds are shown in Scheme 1. **1-Br** was synthesized using reported procedures,[7a]

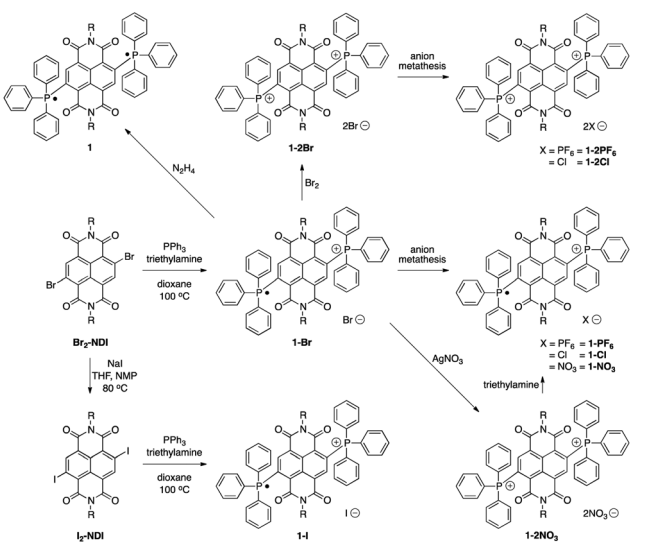

Scheme 1 Syntheses of the BTPP-NDI compounds.

[a]*Institute of Materials Research and Engineering (IMRE), Agency of Science, Technology and Research (A*STAR), 2 Fusionopolis Way, Innovis, #08-03, Singapore 138634, Singapore. E-mail: dexter-tam@imre.a-star.edu.sg*
[b]*Department of Chemistry, National University of Singapore, 3 Science Drive 3, Singapore, 117543, Singapore*

†Electronic supplementary information (ESI) available: Synthesis procedure, characterization data, including X-ray data and NMR spectra. CCDC 1871419–1871426. For ESI and crystallographic data in CIF or other electronic format see DOI: 10.1039/c8qo01122b

‡Both authors contributed equally to the manuscript.

with the solvent replaced by 1,4-dioxane. **1-Br** was oxidized using bromine to give **1-2Br**. **1-PF_6**, **1-2PF_6**, **1-Cl** and **1-2Cl** were obtained *via* anion metathesis. **1-2NO_3** was obtained *via* reacting **1-Br** with silver nitrate, and subsequent reduction using excess triethylamine yielded **1-NO_3**. **Br_2-NDI** was reacted with sodium iodide to give **I_2-NDI**, which can undergo a similar reaction to give **1-I**. Subsequent oxidation of **1-I** with I_2 did not yield the 2+ diiodide. Attempts to obtain **1-2I** using anion metathesis with sodium iodide and **1-2Br** resulted in the formation of **1-I** instead. The neutral compound **1** can be isolated *via* reduction with hydrazine.

X-ray crystallographic analysis

Single crystal XRD structures of all the compounds except **1-2Cl** and **1-NO_3** are shown in Fig. 1 and Fig. S1–S8, ESI.† We were unable to obtain the single crystal XRD structures of **1-2Cl** and **1-NO_3** due to their PET nature (*vide infra*). The anion···π distances were found to be 2.91 Å for **1-PF_6**, 3.15 Å for **1-Cl**, 3.32 Å for **1-Br**, 3.76 Å for **1-I**, 2.81 Å for **1-2PF_6**, 3.19 Å for **1-2Br** and 2.83 Å for **1-2NO_3**. All except **1-I** have anion···π distances shorter than the sum of van der Waals distances between carbon and their respective anion element (F for PF_6^-, N and O for NO_3^-). In general, the 1+ salts displayed longer anion···π distances than their respective 2+ salts due to their weaker anion–π interactions, and the anion···π distances seemed to increase down the group for the halides for both 1+ and 2+ salts. For the multi-nuclear anions, both PF_6^- and NO_3^- showed very short anion···π distances, suggesting the importance of multiple short-contacts for very weakly Lewis basic anions.

X-ray photoelectron spectroscopy (XPS) analysis

The XPS spectra of the BTPP-NDI salts are shown in Fig. S9, ESI.† Peak shifts toward higher binding energies were observed for F 1s (PF_6^-), Cl 2p3/2 (Cl^-), Br 3d5/2 (Br^-) and N 1s (NO_3^-) in 2+ salts as compared to 1+ salts. Higher binding energy species were observed for **1-Cl**, **1-2Cl**, **1-Br**, **1-2Br** and **1-I**, as well as **1-2PF_6**. To the best of our knowledge, such an additional peak for the binding energy of F 1s in PF_6^- is unheard of. The XPS results corroborate the short contacts observed in the single crystal XRD structures, and hence provide strong evidence of anion–π interactions in the solid state for the BTPP-NDI salts.

UV-Vis absorption

The solution UV-Vis absorption spectra of the BTPP-NDI salts in acetonitrile and chloroform are shown in Fig. 2. In polar aprotic solvents like acetonitrile where anion–π interactions are diminished, the anions do not show any observable impact on the λ_{max} for both the 1+ and 2+ salts, except Cl^- in **1-2Cl** that shows absorption peaks corresponding to the 1+ salts, indicating that some form of electron transfer is involved. Saha and co-workers[9] have proposed that very Lewis basic anions like F^- can undergo direct thermal electron transfer to the NDI while Gabbaï *et al.*[10] suggested that F^- deprotonates the solvent (acidified by NDI) and the deprotonated solvent acts as the reducing agent for NDI. Regardless of the mechanism of reduction, the HOMO of Cl^- (−5.54 eV)[11] is not high enough to reduce BTPP-NDI^{2+} (LUMO = −4.75 eV, determined *via* the onset of first reduction in cyclic voltammetry in Fig. S10, ESI†) and Cl^- is not Lewis basic enough (pK_a = −6.3) to deprotonate either acetonitrile (pK_a = 25) or chloroform (pK_a = 15.5). Hence, photoinduced electron transfer (PET) is required to reduce the BTPP-NDI core from 2+ to 1+. PET is known to occur from Cl^- (but not Br^- and I^-) to strongly Lewis π-acidic NDIs due to the stronger Lewis basicity of Cl^-.[9,12] The paramagnetic species arising from PET can also be observed in the broadening of ^{1}H NMR signals of **1-2Cl** (Fig. S21, ESI†). We also noted that there is a difference in the UV-Vis absorp-

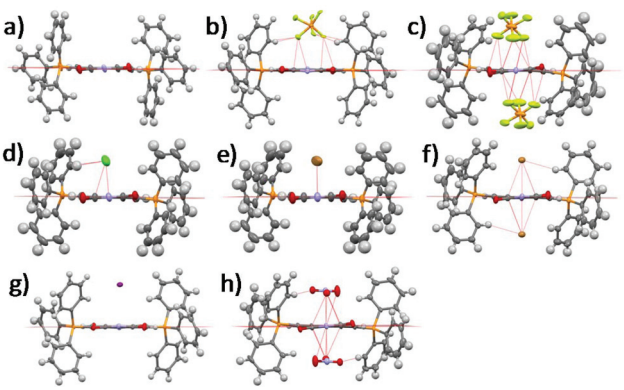

Fig. 1 Single crystal XRD structures of (a) **1**, (b) **1-PF_6**, (c) **1-2PF_6**, (d) **1-Cl**, (e) **1-Br**, (f) **1-2Br**, (g) **1-I** and (h) **1-2NO_3**. Solvent molecules and alkyl groups are omitted for clarity.

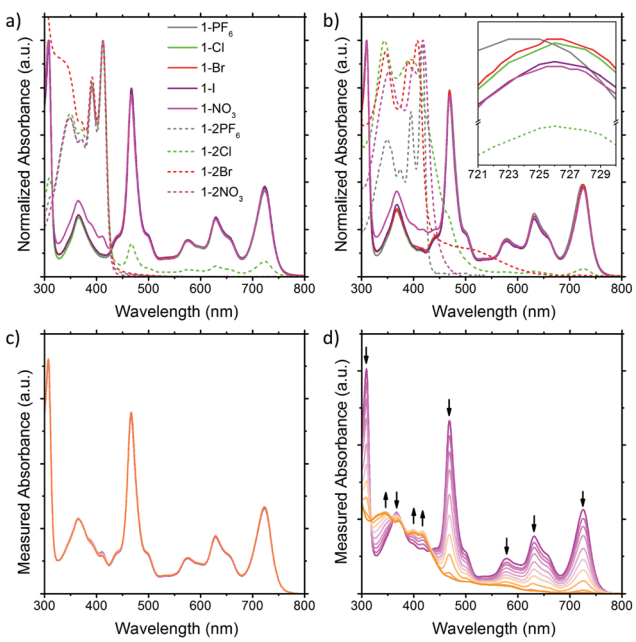

Fig. 2 Solution UV-Vis of the BTPP-NDI salts in (a) acetonitrile and (b) chloroform. Solution UV-Vis of **1-NO_3** in (c) acetonitrile and (d) chloroform upon illumination.

tion of **1-NO$_3$** as compared to that of the other 1+ salts from 320 to 430 nm.

In nonpolar solvents where anion–π-radical interactions are expected to be stronger, the λ_{max} values of the 1+ halide and nitrate salts were red-shifted from 723 nm in acetonitrile to about 726 nm in chloroform. In contrast, the λ_{max} of **1-PF$_6$** was only red-shifted from 723 nm in acetonitrile to 724 nm in chloroform. This miniscule shift for halide and nitrate salts as compared to that of **1-PF$_6$** is probably due to electronic interactions between the frontier orbitals of the anions and the SUMO of the radical cation arising from their similar energy levels (Fig. S44, ESI†) when the cation and anion are in close proximity, which is also supported by TDDFT calculations (Fig. S13 and Table S5, ESI†). The difference in the UV-Vis absorption of **1-NO$_3$** as compared to the other 1+ salts from 320 to 430 nm remained observable in chloroform. For the 2+ salts, their absorption profiles in chloroform are largely different from those in acetonitrile, with the exception of **1-2PF$_6$** and **1-2NO$_3$** due to their electrochemical inactivity towards the 2+ cation for the latter. For **1-2Cl**, the absorption peaks corresponding to the 1+ salts remain due to PET (*vide supra*). For **1-2Br**, a charge transfer band at around 520 nm, arising from the stronger anion–π interaction in chloroform, was observed.

Based on time-dependent density functional theory (TDDFT) calculations, the lowest energy $D_0 \rightarrow D_1$ transition for the 1+ salts is mainly contributed by SOMOα → LUMOα (Table S5, ESI†). With the SUMO value estimated to be −4.75 eV from CV measurements and an optical bandgap of 1.65 eV for the 1+ salts, the LUMO value of the 1+ salts is estimated to be −3.10 eV. Based on the reduction potential of NO_3^- ($NO_3^- + 2H^+ + 2e^- \rightarrow NO_2^- + 2H_2O$, E° = +0.42 V;[13] Fc/Fc$^+$ *vs.* SHE = +0.62 V;[14] HOMO of Fc = 4.8 eV; LUMO = −4.60 eV) we postulate that **1-NO$_3$** will undergo "reverse" PET, *i.e.*, π → anion PET *cf.* anion → π "normal" PET reported by Saha and co-workers (see the energy diagram in Fig. S44, ESI†).[9] Upon illumination, the UV-Vis absorption of **1-NO$_3$** remained similar in acetonitrile but degraded rapidly in chloroform, giving rise to two new peaks at ~400 nm corresponding to the 2+ cation and a new peak at 350 nm corresponding to the 2+ cation and NO_2^- (Fig. 2c & d).[15] Based on these observations, we reasoned that the pK_a values of the solvents are the likely cause for the distinct stability of **1-NO$_3$**. As stated in the redox equation, the reduction of NO_3^- requires the presence of H^+, which is promoted by the much higher acidity of chloroform as compared to acetonitrile.

Nuclear magnetic resonance (NMR) and electron paramagnetic resonance (EPR)

To further characterize the BTPP-NDI salts, their halogen NMR spectra were collected (Fig. S27–S38, ESI†) and their chemical shifts (δ) and linewidths at the half peak height ($LW_{1/2}$) were tabulated (Table S3, ESI†). Unfortunately, we were not able to perform ^{14}N NMR due to the unavailability of the required NMR probe. Respective tetrabutylammonium salts (TBA-X) were used as the control. Restricted motion (^{19}F) and boundedness (^{35}Cl, ^{81}Br and ^{127}I) often result in a broader $LW_{1/2}$ for their NMR signals.[16] In polar aprotic solvents like acetonitrile-d_3, the anions in TBA.X salts behave like free ions and hence sharp halogen NMR signals were observed. The ^{19}F NMR signals for **1-2PF$_6$** showed a very narrow $LW_{1/2}$ (1.5 Hz) and were essentially the same as the control while **1-PF$_6$** showed a slightly broader $LW_{1/2}$ (1.9 Hz). For **1-Cl**, the $LW_{1/2}$ of the ^{35}Cl NMR signal was 63 Hz while **1-2Cl** did not show any observable signal. Similarly, the $LW_{1/2}$ of the ^{81}Br NMR signal for **1-Br** was 915 Hz while **1-2Br** did not show any observable signal. The broadening of the ^{35}Cl and ^{81}Br NMR signals in **1-Cl** and **1-Br** as compared to their TBA.X salts suggests that Cl^- and Br^- are somewhat bound to the BTPP-NDI core. Similarly, the absence of the ^{35}Cl and ^{81}Br NMR signals in **1-2Cl** and **1-2Br** suggests that Cl^- and Br^- are strongly bound, or due to the occurrence of PET for the former, resulting in the NMR signals being too broad to be observed. No ^{127}I NMR signal could be observed for **1-I** due to the large nuclear quadrupole moment ($I > 5/2$). Although the $LW_{1/2}$ of halogen NMR can be used to estimate the restricted motion/boundedness of the halides, the presence of paramagnetic radical species further complicates matters. This is because apart from the omnipresence of diamagnetic relaxation, paramagnetic compounds also exhibit paramagnetic relaxation which involves several contributions that make estimation difficult.[17]

Based on the solution UV-Vis absorption, acetonitrile is able to provide effective electrostatic screening in the 1+ salts *via* its high dielectric constant of 37.5. However, it has a very small magnetic susceptibility of -2.8×10^{-5} cm^3 mol^{-1}; hence it is unable to provide effective magnetostatic screening. Thus, deviations from the halogen δ of TBA.X are most likely caused by magnetic spin polarization induced by the π-radical. The $\Delta\delta$ with respect to TBA.X are 18.8 Hz for **1-PF$_6$**, 114.4 Hz for **1-Cl** and 389.8 Hz for **1-Br**. Thus, the degree of the anion–π-radical interaction for the 1+ salts is **1-Br** > **1-Cl** > **1-PF$_6$**. In nonpolar solvents like chloroform-*d*, the anions should be more strongly bound and hence we expect broader halogen NMR signals. The $LW_{1/2}$ of the ^{19}F NMR signal for **1-PF$_6$** (162.5 Hz) is more than two orders of magnitude larger than the control (1.5 Hz) as shown in Fig. 3. The $LW_{1/2}$ of the ^{19}F NMR signal for **1-2PF$_6$** (4.4 Hz) is only about three times larger than the control. It is thus clear that the very broad $LW_{1/2}$ for **1-PF$_6$** in chloroform-*d* was caused by stronger magnetic spin polarization arising

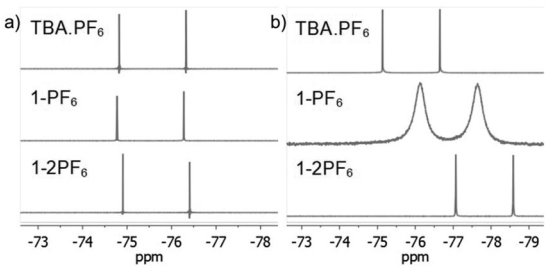

Fig. 3 ^{19}F NMR of the PF_6^- salts in (a) acetonitrile-d_3 and (b) chloroform-*d*.

from the stronger anion–π-radical interaction between PF_6^- and the π-radical. Similar ^{19}F NMR signal broadening was previously reported, but in a selenium-centered radical SbF_6^- salt.[18] To our knowledge, there is no report on such ^{19}F NMR signal broadening in solution with π-radicals. The observed $LW_{1/2}$ of the ^{35}Cl NMR signal for **1-Cl** was 415 Hz while no ^{81}Br NMR signal for **1-Br** could be observed. Similarly, no ^{35}Cl and ^{81}Br NMR signals could be observed for **1-2Cl** and **1-2Br**. The $LW_{1/2}$ trend of the halogen NMR signals is in agreement with the polarizabilities of the anions and the polarizing power of the cations.

EPR of the 1+ salts was measured in dry dichloromethane (Fig. S10, ESI†). The 1+ halides did not show any noticeable difference while **1-NO$_3$** showed a broader signal, indicating some exchange interaction between the BTPP-NDI radical cation and NO_3^-. We believe that this difference in the EPR signal for **1-NO$_3$**, together with the difference in its UV-Vis absorption, is caused by strong anion–π-radical interactions, as shown by the unexpected short anion···π distance calculated using DFT (2.93 Å, Table S4, ESI,† *vide infra*). The difference in the EPR signal and UV-Vis absorption for **1-NO$_3$** is also supported by the Lewis basicity of the anions, based on the pK_a of their respective acids: HPF_6 < HI < HBr < HCl < HNO_3.

Electrospray ionization-mass spectrometry (ESI-MS)

The presence of anion–π/anion–π radical interactions in BTPP-NDI salts was also supported by electrospray ionization mass spectrometry (ESI-MS) data. Peaks corresponding to *m*/*z* values of 1157.41 $[1 + PF_6]^+$ were found for **1-PF$_6$** and **1-2PF$_6$**; 1047.42 $[1 + Cl]^+$ for **1-Cl** and **1-2Cl**; 1091.37 $[1 + Br]^+$ for **1-Br** and **1-2Br**; and 1074.21 $[1 + NO_3]^+$ for **1-NO$_3$** and **1-2NO$_3$** (Fig. S39–S42, ESI†). However, $[1 + I]^+$ could not be observed in **1-I** as most of the I^- was oxidized to I_3^- in the ESI-MS, which does not have any significant anion–π/anion–π radical interactions with BTPP-NDI, consistent with our previous findings from the pyridinium–NDI system[11] (Fig. S43, ESI†).

Density functional theory (DFT) calculations

To provide molecular interpretation for the halogen NMR, we performed density functional theory (DFT) calculations by employing long-range corrected hybrid functional CAMB3LYP[19] with Pople-type basis 6-311G+(d,p) for atoms in the cation and LANL2DZdp[20] for atoms in the anion. The optimized structures agree very well (<5% deviation) with the obtained single crystal structures (refer to Table S4 in the ESI† for the experimental and calculated bond lengths), with exceptions to the larger calculated anion···π distances (>5% deviation) for the 1+ halides. This systematic overestimation of the anion···π distances for the 1+ halides is likely the consequence of electron self-interactions, leading to over-stabilization of the coulombic terms relative to the exchange–correlation terms, a situation similar to a two-center three-electron system.[21] All anion···π distances calculated for 1+ salts were larger than those of the corresponding 2+ salts except for **1-NO$_3$** (2.933 Å) which showed a smaller value than that of **1-2NO$_3$** (2.964 Å), with the former in an edge-on configuration and the latter in a face-on configuration agreeing with the single crystal structure. We believe that the shortest anion···π distance for **1-NO$_3$** among the 1+ salts is the likely explanation for its different UV-Vis absorption and EPR as compared to the other 1+ salts. The edge-on configuration for **1-NO$_3$** is in agreement with the absorbed nitrate on various metal electrodes during reduction.[22] In **1-2NO$_3$**, the interaction between the highly π-acidic BTPP-NDI core and the π-rich NO_3^- in the face-on configuration is very favorable. In **1-NO$_3$**, the BTPP-NDI core is relatively π-rich and hence to minimize electronic repulsion, the edge-on configuration is favored. The different configurations of NO_3^- on the π-acidic BTPP-NDI core support the concepts used in anion–π catalysis, *e.g.*, stabilization of nitronate intermediates in enamine chemistry.[3,23] The 1+ salts show non-zero spin densities on the anions with Br^- > Cl^- > PF_6^- > I^- > NO_3^- (Fig. 4a). This is in accordance with the trend of anion–π-radical interactions based on the $\Delta\delta$ in the halogen NMR (*vide supra*). Even though PF_6^- is very weakly polarizable, there is a significant amount of delocalized spin density that accounts for the severe broadening of the ^{19}F NMR signal for **1-PF$_6$**. The significant amount of the delocalized spin density on PF_6^- arises from the fact that PF_6^- has short anion···π distances and the strength of the magnetostatic field (from the π-radical) obeys an inverse-cube law with respect to the distance. Hence, even the highly polarizable I^- showed the least spin density due to its large anion···π distance.

It is also worth noting that the spin densities on the 1+ radical and the halides/NO_3^- are of the same spin type while being of different spin types for PF_6^-. Even when considering a C_i symmetry point group with an additional anion, *i.e.* 1-X + X^-, the trend of the spin density remains the same. The same spin type in *m*-phenylene-based bis(aminoxyl) diradical–anion complexes was believed to enhance the intramolecular ferromagnetic exchange interaction between the diradicals.[8a] In the case of our BTPP-NDI system, the same spin type may facilitate intermolecular ferromagnetic exchange interactions in single crystals for the halide salts while antiferromagnetic exchange interactions may be observed in the single crystal for **1-PF$_6$** due to its different spin types. In the solid state, the intermolecular antiferro/ferromagnetic exchange interactions are expected to be stronger due to the stronger anion–π radical

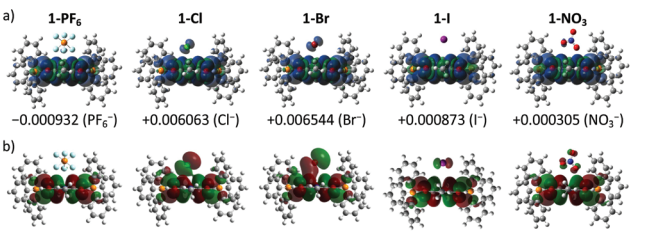

Fig. 4 (a) Spin density (isovalue = 0.0001 e^-/au^3) and (b) SOMO (isovalue = 0.01 e^-/au^3) of the geometry optimized 1+ salts in the gas phase using DFT UCAMB3LYP 6-311G+(d,p) for atoms in the cation and LANL2DZ with polarization and diffuse functions for atoms in the anion. Numerical values denote the sum of Mulliken atomic spin densities on anions.

interactions as shown in the XPS data (Fig. S10†). Magnetic measurements of the single crystals are currently underway.

The strength of the electrostatic field (arising from the coulombic attraction between the cation and anion) obeys an inverse-square law with respect to the distance. This means that even though the magnetic polarization of I^- is weak in **1-I**, the electric polarization is stronger. This is true for all anions and is reflected in the SOMO in Fig. 4b. The polarizable halides and NO_3^- show significant contribution to the SOMO while the very weakly polarizable PF_6^- shows negligible contribution. Furthermore, the trend of the calculated λ_{max} calculated *via* TDDFT (Fig. S13 and Table S5, ESI†) is in accordance with the experimentally observed UV-Vis absorption. This explains the red-shifted λ_{max} for **1-Cl**, **1-Br**, **1-I** and **1-NO_3** as compared to **1-PF_6** in chloroform.

Conclusions

In conclusion, we extend the concept of anion–π interactions to anion–π-radical interactions. We note that even in solution, anions are able to induce changes in the photophysical and magnetic properties of the cationic π-radical. Apart from the "normal" PET from the anion to the Lewis π-acidic 2+ cation for **1-2Cl**, we were able to observe a "reverse" PET from the radical cation to the anion for **1-NO_3**. The radical cation is also able to induce magnetic spin polarization of the anions in NMR. These effects should be much stronger in the solid state without the electrostatic screening from the solvent molecules. We believe that our results will provide better understanding of organic ferromagnets and p-doped conductors.

Conflicts of interest

There are no conflicts to declare.

Acknowledgements

We like to thank Ms Tan Geok Kheng (X-ray Diffraction Laboratory in National University of Singapore) and Ms Debbie Seng (Structural Materials Department in IMRE) for their efforts to solve the single crystal structures and collect the XPS data.

Notes and references

1 (*a*) D.-X. Wang and M.-X. Wang, *J. Am. Chem. Soc.*, 2013, **135**, 892–897; (*b*) M. M. Watt, L. N. Zakharov, M. M. Haley and D. W. Johnson, *Angew. Chem., Int. Ed.*, 2013, **52**, 10275–10280.

2 (*a*) L. Adriaenssens, C. Estarellas, A. Vargas Jentzsch, M. Martinez Belmonte, S. Matile and P. Ballester, *J. Am. Chem. Soc.*, 2013, **135**, 8324–8330; (*b*) M. Giese, M. Albrecht and K. Rissanen, *Chem. Commun.*, 2016, **52**, 1778–1795.

3 (*a*) Y. Zhao, C. Beuchat, Y. Domoto, J. Gajewy, A. Wilson, J. Mareda, N. Sakai and S. Matile, *J. Am. Chem. Soc.*, 2014, **136**, 2101–2111; (*b*) Y. Zhao, Y. Cotelle, L. Liu, J. López-Andarias, A.-B. Bornhof, M. Akamatsu, N. Sakai and S. Matile, *Acc. Chem. Res.*, 2018, **51**, 2255–2263.

4 (*a*) C.-Z. Li, C.-C. Chueh, F. Ding, H.-L. Yip, P.-W. Liang, X. Li and A. K.-Y. Jen, *Adv. Mater.*, 2013, **25**, 4425–4430; (*b*) B. Lüssem, C.-M. Keum, D. Kasemann, B. Naab, Z. Bao and K. Leo, *Chem. Rev.*, 2016, **116**, 13714–13751; (*c*) X. Zhao, D. Madan, Y. Cheng, J. Zhou, H. Li, S. M. Thon, A. E. Bragg, M. E. DeCoster, P. E. Hopkins and H. E. Katz, *Adv. Mater.*, 2017, **29**, 1606928; (*d*) Y. Xu, J. Yuan, J. Sun, Y. Zhang, X. Ling, H. Wu, G. Zhang, J. Chen, Y. Wang and W. Ma, *ACS Appl. Mater. Interfaces*, 2018, **10**, 2776–2784.

5 (*a*) J.-L. Brédas and G. B. Street, *Acc. Chem. Res.*, 1985, **1985**, 309–315; (*b*) H. Fukutome, A. Takahashi and M.-a. Ozaki, *Chem. Phys. Lett.*, 1987, **133**, 34–38; (*c*) P. Bujak, I. Kulszewicz-Bajer, M. Zagorska, V. Maurel, I. Wielgus and A. Pron, *Chem. Soc. Rev.*, 2013, **42**, 8895–8999.

6 D. M. d. Leeuw, M. M. J. Simenon, A. R. Brown and R. E. F. Einerhand, *Synth. Met.*, 1997, **87**, 53–59.

7 (*a*) S. Kumar, M. R. Ajayakumar, G. Hundal and P. Mukhopadhyay, *J. Am. Chem. Soc.*, 2014, **136**, 12004–12010; (*b*) Q. Song, F. Li, Z. Wang and X. Zhang, *Chem. Sci.*, 2015, **6**, 3342–3346; (*c*) S. K. Keshri, S. Kumar, K. Mandal and P. Mukhopadhyay, *Chem. – Eur. J.*, 2017, **23**, 11802–11809; (*d*) S. Debnath, C. J. Boyle, D. Zhou, B. Wong, K. R. Kittilstved and D. Venkataraman, *RSC Adv.*, 2018, **8**, 14760–14764; (*e*) A. J. Greenlee, C. K. Ofosu, Q. Xiao, M. M. Modan, D. E. Janzen and D. D. Cao, *ACS Omega*, 2018, **3**, 240–245; (*f*) Z. Bin, H. Guo, Z. Liu, F. Li and L. Duan, *ACS Appl. Mater. Interfaces*, 2018, **10**, 4882–4886.

8 (*a*) M. E. Ali and P. M. Oppeneer, *J. Phys. Chem. Lett.*, 2011, **2**, 939–943; (*b*) D. Bhattacharya, S. Shil, A. Misra, L. Bytautas and D. J. Klein, *J. Phys. Chem. A*, 2016, **120**, 9117–9130.

9 S. Guha, F. S. Goodson, L. J. Corson and S. Saha, *J. Am. Chem. Soc.*, 2012, **134**, 13679–13691.

10 G. Bélanger-Chabot, A. Ali and F. P. Gabbaï, *Angew. Chem., Int. Ed.*, 2017, **56**, 9958–9961.

11 T. L. D. Tam, C. K. Ng, X. Lu and J. Wu, *Chem. Commun.*, 2018, **54**, 7374–7377.

12 S. Saha, *Acc. Chem. Res.*, 2018, **51**, 2225–2236.

13 B. C. Berks, S. J. Ferguson, J. W. B. Moir and D. J. Richardson, *Biochim. Biophys. Acta, Bioenerg.*, 1995, **1232**, 97–173.

14 V. V. Pavlishchuk and A. W. Addison, *Inorg. Chim. Acta*, 2000, **298**, 97–102.

15 J. Mack and J. R. Bolton, *J. Photochem. Photobiol., A*, 1999, **128**, 1–13.

16 (*a*) C. Hall, *Q. Rev., Chem. Soc.*, 1971, **25**, 87–109; (*b*) J.-X. Yu, R. R. Hallac, S. Chiguru and R. P. Mason, *Prog. Nucl. Magn. Reson. Spectrosc.*, 2013, **70**, 25–49.

17 J. Koehler and J. Meiler, *Prog. Nucl. Magn. Reson. Spectrosc.*, 2011, **59**, 360–389.
18 S. Zhang, X. Wang, Y. Su, Y. Qiu, Z. Zhang and X. Wang, *Nat. Commun.*, 2014, **5**, 4127, DOI: 4110.1038/ncomms5127.
19 T. Yanai, D. P. Tew and N. C. Handy, *Chem. Phys. Lett.*, 2004, **393**, 51–57.
20 C. E. Check, T. O. Faust, J. M. Bailey, B. J. Wright, T. M. Gilbert and L. S. Sunderlin, *J. Phys. Chem. A*, 2001, **105**, 8111–8116.
21 B. Braïda, P. C. Hiberty and A. Savin, *J. Phys. Chem. A*, 1998, **102**, 7872–7877.
22 (*a*) M. C. P. M. da Cunha, M. Weber and F. C. Nart, *J. Electroanal. Chem.*, 1996, **414**, 163–170; (*b*) S.-E. Bae, K. L. Stewart and A. A. Gewirth, *J. Am. Chem. Soc.*, 2007, **129**, 10171–10180; (*c*) K. Nakata, Y. Kayama, K. Shimazu, A. Yamakata, S. Ye and M. Osawa, *Langmuir*, 2008, **24**, 4358–4363.
23 (*a*) Y. Zhao, Y. Domoto, E. Orentas, C. Beuchat, D. Emery, J. Mareda, N. Sakai and S. Matile, *Angew. Chem., Int. Ed.*, 2013, **52**, 9940–9943; (*b*) Y. Zhao, S. Benz, N. Sakai and S. Matile, *Chem. Sci.*, 2015, **6**, 6219–6223; (*c*) J. López-Andarias, A. Frontera and S. Matile, *J. Am. Chem. Soc.*, 2017, **139**, 13296–13299.